Inland Waters

ISSN: 2044-2041 (Print) 2044-205X (Online) Journal homepage: http://www.tandfonline.com/loi/tinw20

Phytoplankton community structure and succession in karst cascade reservoirs, SW China

Baoli Wang, Xiao-Long Qiu, Xi Peng & Fushun Wang

To cite this article: Baoli Wang, Xiao-Long Qiu, Xi Peng & Fushun Wang (2018): Phytoplankton community structure and succession in karst cascade reservoirs, SW China, Inland Waters, DOI: 10.1080/20442041.2018.1443550

To link to this article: https://doi.org/10.1080/20442041.2018.1443550

INLAND WATERS, 2018
https://doi.org/10.1080/20442041.2018.1443550

Phytoplankton community structure and succession in karst cascade reservoirs, SW China

Baoli Wang,[a,b] Xiao-Long Qiu,[b,c] Xi Peng,[b] and Fushun Wang[d]

[a]Institute of Surface-Earth System Sciences, Tianjin University, Tianjin, China; [b]State Key Laboratory of Environmental Geochemistry, Institute of Geochemistry, Chinese Academy of Sciences, Guiyang, China; [c]University of Chinese Academy of Sciences, Beijing, China; [d]Institute of Applied Radiation, School of Environmental and Chemical Engineering, Shanghai University, Shanghai, China

ABSTRACT

Cascade reservoir-river systems evolve to become a new ecological region produced by anthropogenic disturbances. Systematic studies of spatial–temporal patterns of phytoplankton community structure are still lacking in these systems, and thus we investigated phytoplankton composition and related environmental factors in the impounded Wujiang River, southwest China. The results showed that the dominant groups were Chlorophyta, Bacillariophyta, and Cyanophyta, whereas Pyrrhophyta and Cryptophyta mainly appeared from May to August. Bacillariophyta were dominant algae in the river water, Cyanophyta in the eutrophic reservoirs, and Chlorophyta, Bacillariophyta, and Cyanophyta were dominant in the mesotrophic reservoirs. Water temperature was an important limiting factor for algal growth, and algal biomass produced 2 peak values in May and in August. Backpropagation artificial neural networks (BPANNs) have accurately predicted time-series variation of dominant algal abundance. The sensitivity analyses indicated that water temperature, dissolved CO_2, and silicon were the main factors influencing phytoplankton community structure, suggesting algal succession is constrained by carbon and silicon biogeochemical cycles. Results suggested that Cyanophyta used HCO_3^- as an inorganic carbon source when the CO_2 concentration was less than ~10 μmol L^{-1}, leading to the species succession from Bacillariophyta to Cyanophyta.

ARTICLE HISTORY
Received 3 August 2017
Accepted 18 February 2018

KEYWORDS
BPANNs model; carbon; phytoplankton; silicon; Wujiang River

Introduction

Phytoplankton community succession is influenced by several environmental factors. An increase in water turbulence may result in changes from cyanobacteria (Cyanophyta) to green algae (Chlorophyta) and diatoms (Bacillariophyta; e.g., Reynolds et al. 1983, Harris and Baxter 1996), and a decrease in temperature can also lead to a distinct shift from nitrogen-fixing cyanobacteria toward diatoms (Markensten et al. 2010, Schabhuttl et al. 2013). Furthermore, nutrient stoichiometry such as carbon:silicon and phosphorus:silicon ratios can influence the succession between diatom and nondiatom phytoplankton (Wang et al. 2014, 2016).

Damming for hydropower generation is one of the most significant human activities affecting natural rivers. Hydropower reservoirs have the characteristics of not only temperature and nutrient stratifications, but also artificial regulation such as releasing water from the bottom of the dam and anti-seasonal storage of water (Serra et al. 2007, Wang et al. 2014). The impounded rivers evolve and form their own hydrological characteristics, elemental biogeochemical cycles, and phytoplankton ecology; therefore, the impounded rivers can be considered a new ecological region produced by anthropogenic disturbances.

Karst hydropower reservoirs are usually canyon reservoirs with high concentrations of dissolved inorganic carbon. Systematic studies of spatial–temporal patterns of phytoplankton community structure are still lacking in karst cascade reservoirs. We hypothesize that in these reservoirs algal succession relates to the carbon geochemical cycle. Here we investigated phytoplankton community structure and related environmental variables in the impounded Wujiang River, southwest China, to test our hypothesis.

Methods

Study area

As a typical impounded river, the Wujiang River, the largest river in Guizhou Province, is particularly well suited for

CONTACT Baoli Wang baoli.wang@tju.edu.cn

this study. It is a southern tributary of the Changjiang River with a length of 1037 km, a fall of 2124 m, a drainage area of 8.8×10^4 km^2, and an average runoff of 53.4×10^9 m^3 per year. Since 1959, a series of reservoirs have been constructed along this river, and the main hydrological features of these reservoirs are well understood (Wang et al. 2013). We investigated 9 stations in this study (Fig. 1), 4 of which (W1, W2, W6, and W7) were selected for backpropagation artificial neural networks (BPANNs) modeling. W1 is located at the Liuchong River and represents a primal river, whereas W6 represents a river influenced by damming. Hongjiadu Reservoir (W2) is a young reservoir, and Wujiangdu Reservoir (W7) is an old reservoir.

Sampling and analytical methods

Surface water samples (upper 0.5 m) were collected twice a month from May 2011 to May 2012. Water temperature (T), dissolved oxygen (DO), and pH were measured *in situ* using a calibrated water quality probe (model YSI 6600). A small portion of each sample was stored for analyses of total nitrogen (TN) and total phosphorus (TP). Both were determined spectrophotometrically (Unico UV-2000) after alkaline potassium persulfate digestion (EPA 1988). Samples for major cations and anions were filtered through 0.45 μm filters. Samples for cation analysis were acidified to pH 2 with ultrapurified HNO_3. Major cations of calcium, magnesium, potassium, and sodium (Ca^{2+}, Mg^{2+}, K^+, and Na^+) and dissolved silicon (DSi) were analysed by inductively coupled plasma optical emission spectrometer (ICP-OES, USA), and anions sulfate, nitrate, and chloride (SO_4^{2-}, NO_3^-, and Cl^-) by high performance liquid chromatography ICS-90 (Dionex, USA). These major ions were used to calculate ionic strength. Alkalinity was titrated with HCl on site. Dissolved carbon dioxide (CO_2) concentration was calculated from alkalinity, pH, and T

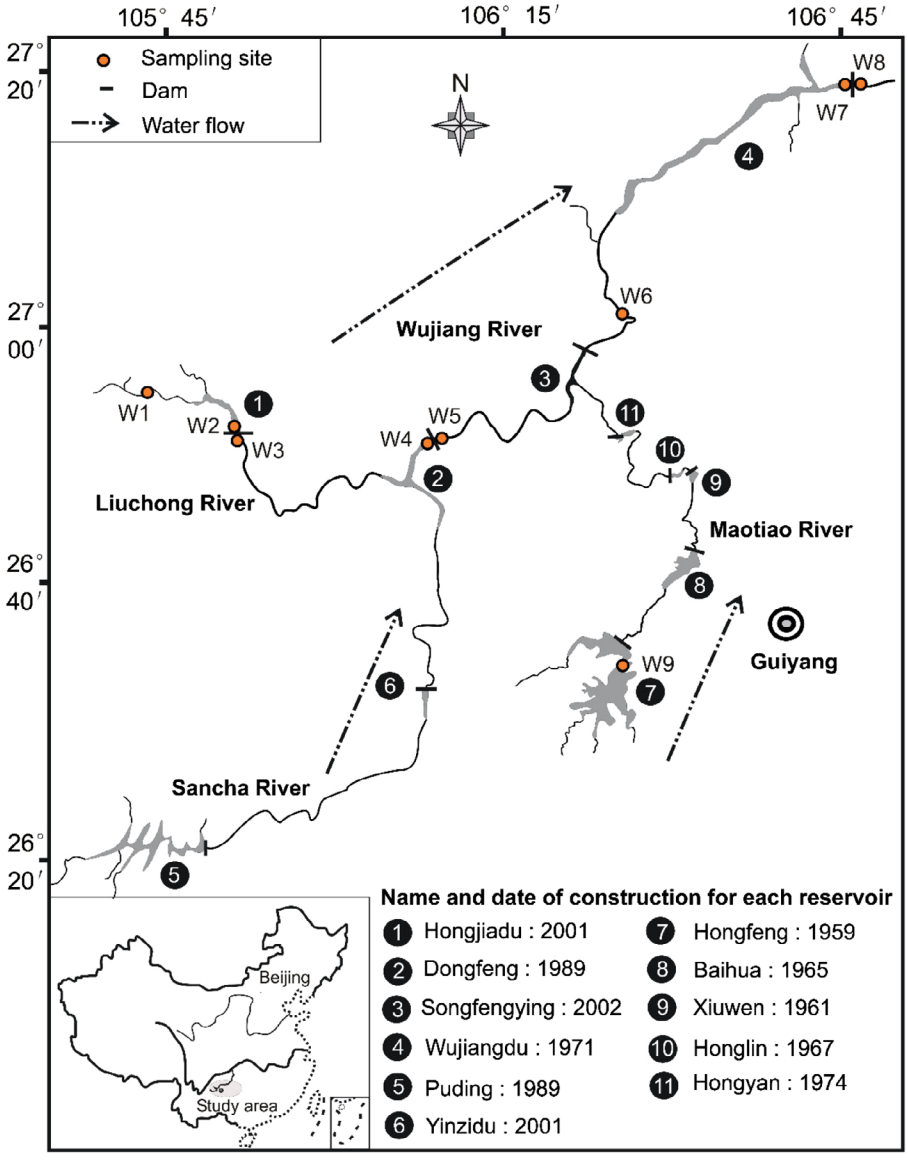

Figure 1. Position of reservoirs and sampling locations on the Wujiang River, southwest China.

with corrections of dissociation constants by temperature and ionic strength (Maberly 1996). A 1.5 L surface water sample was preserved with Lugol's solution for quantitative analysis of phytoplankton. Phytoplankton for qualitative analysis was collected with a 64 μm nylon mesh and preserved with formaldehyde solution (2% final concentration). The method of Zhang and Huang (1991) was used for taxon identification, counting, and cell dimensions using a standard light microscope. The biovolume of each species was geometrically calculated (Hillebrand et al. 1999), and the wet weight (mg L^{-1}) of phytoplankton biomass was calculated according to its biovolume and cell density (Zhang and Huang 1991). Chlorophyll (Chl) content was determined using a calibrated Walz PHYTO-PAM-ED pulse amplitude modulated fluorescence system with PHYTO-WIN software 2.13 (Heinz Walz GmbH, Effeltrich, Germany). Pearson's correlation coefficient analysis was carried out with software SPSS 11.5 (SPSS, Inc.).

Back propagation artificial neural network architecture for modeling

BPANNs were developed from a learning procedure reported by Rumelhart et al. (1986) and proved successful for modeling phytoplankton dynamics characterized by nonlinearity and complexity in aquatic ecosystems (Recknagel 1997, Wei et al. 2001, Jeong et al. 2006). The structure of a BPANN consisted of 3 layers: an input, a hidden layer, and an output layer. TN, TP, DSi, dissolved CO_2, T, pH, and DO were the external inputs, and cell densities of different phytoplankton groups were the outputs. Data for each month were divided into 2 sets. Data from the first semi-month made up the training database, which was assumed to contain the information necessary to establish the relation between the input layer and the output layer (Lek and Guegan 1999), and were used to train the BPANNs and build the models. Data from the second semi-month constituted test sets used to validate the BPANN models. The sigmoid function: $f(x) = 1/(1+e^{-x})$ was chosen to estimate the activation level in the hidden layer. The learning rate of BPANNs was 0.05, and the momentum constant (mc = 0.9) and a training goal (1e-3) were used. By repeatedly training and validating, the best performing BPANN was selected for sensitivity analysis to identify the sensitivity of phytoplankton cell density to the change of each input factor. Input parameters increasing and decreasing by 10% were fed to the selected network, and the output values were compared with the output values calculated by feeding the network with observed input parameters. The calculations were performed by MATLAB 7.8 (Minitab, Inc.).

Results

Basic physical, chemical, and biological properties

Major physical, chemical, and biological variables are presented in Fig. 2 and Table 1. T showed clear monthly variations, increasing from February and peaking in August (Fig. 2a–b). Amplitude of T with time was larger than with space while that of pH showed a reverse tendency. Generally, pH decreased along the main Wujiang River, and values were lower downstream than upstream of the dam. DO displayed the reverse temporal variation compared to T and a similar spatial variation to pH. Temperature, pH, and DO (Fig. 2c–f) showed significant correlations with each other (Table 2).

The average values of dissolved CO_2, TN, TP, DSi, and Chl showed small monthly fluctuations but displayed relatively large amplitudes among stations (Fig. 2g–n). High CO_2 concentrations were recorded downstream of the dam and low DSi concentrations upstream of the dam. The reservoirs Wujiangdu (W7) and Hongfeng (W9) showed high Chl contents, suggesting their trophic level was high. Chl content showed significant negative correlations to TN, CO_2, and DSi (Table 2). TN in the Hongfeng reservoir had the lowest value because the TN concentration in the Maotiao River is lower than the concentration in the Wujiang River.

Phytoplankton

We recorded 7 algal groups in this river–reservoir system (Fig. 3). The dominant groups were Chlorophyta, Bacillariophyta, and Cyanophyta, whereas Pyrrhophyta and Cryptophyta mainly appeared from May to August. Generally, Bacillariophyta were dominant in the river waters, whereas Cyanophyta were dominant in the eutrophic reservoirs Hongfeng and Wujiangdu. The 3 main algal groups coexisted in the mesotrophic reservoirs Hongjiadu and Dongfeng. Biomass of the total algae and most algal groups presented 2 peak values in May and in August, and the phytoplankton community structure varied markedly with time and space (Fig. 2o–x and 3).

Dynamics of different phytoplankton groups predicted by BPANN models

The predicted output values showed a significant correlation with the measured values, indicating that the timing of the predicted output values compared well with the measured data (Fig. 4). The simulation results showed different patterns among the different stations, and the magnitude of the dominant algal groups in the 4 stations was also well predicted. Predictions of the dominant algal

groups were usually more accurate than those of nondominant groups.

Sensitivity analyses of the BPANN models conducted to determine the sensitivity of algal groups to different environmental factors (Tables 3 and 4) found that the dominant Cyanophyta in stations W2 and W7 were highly sensitivity to T, CO_2, and pH. The dominant Bacillariophyta in stations W1, W2, and W6 were sensitive to T, CO_2, pH, and DSi, and the dominant Chlorophyta in station W2 were sensitive to T and pH.

Discussion

Factors limiting phytoplankton growth

A hydropower reservoir changes the hydrology, transparency, and nutrient cycling compared with the original

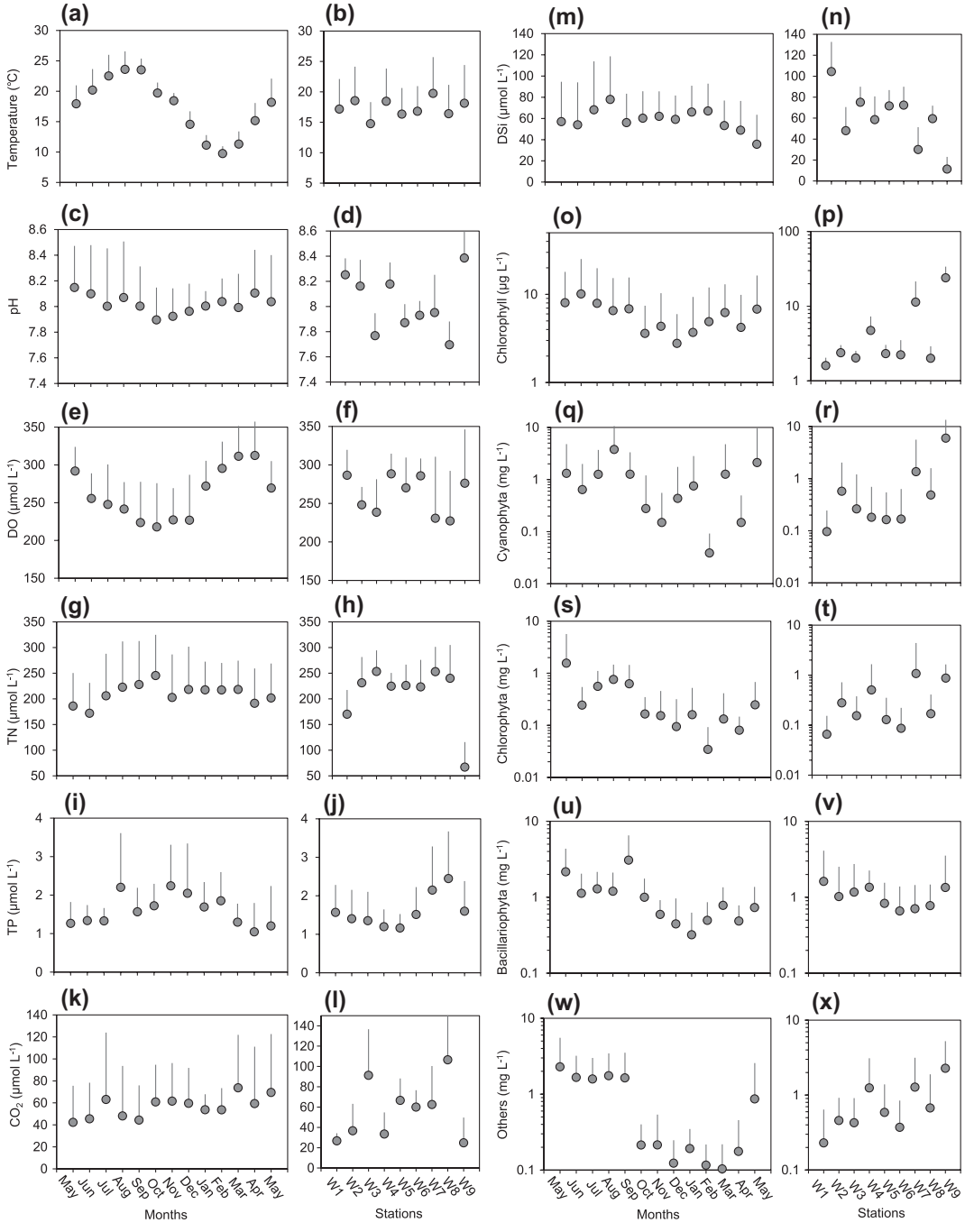

Figure 2. Physical, chemical, and biological variables at different stations on the Wujiang River, southwest China, from May 2011 to May 2012. Station locations refer to Fig. 1. Values are shown as average and positive standard deviation, and phytoplankton biomass as mg wet weight per L.

Table 1. Averages and range of major biogeochemical variables in this study (n = 234). T = water temperature; DO = dissolved oxygen; TN = total nitrogen; TP = total phosphorus; CO_2 = dissolved CO_2; DSi = dissolved silicon; Chl = chlorophyll.

			DO	CO_2	TN	TP	DSi	
	T (°C)	pH			(μmol L^{-1})			Chl (μg L^{-1})
Aver	17.37	7.92[a]	261.2	56.5	209.8	1.60	58.9	5.84
SD	5.17	0.31	53.9	40.0	72.8	0.89	31.9	8.49
Max	29.66	8.99	389.7	226.9	426.3	5.81	152.7	49.29
Min	6.62	7.36	98.4	2.1	7.2	0.38	0.02	0.92

[a]Average calculated from the geometric average; the arithmetic average was 8.02.

Table 2. Results of Pearson's correlation coefficient analysis. T = water temperature; DO = dissolved oxygen; TN = total nitrogen; TP = total phosphorus; CO_2 = dissolved CO_2; DSi = dissolved silicon; Chl = chlorophyll.

	pH	DO	TN	TP	CO_2	DSi	Chl
T	0.239**	−0.335**	−0.063	0.034	−0.300**	−0.151*	0.272**
pH		0.561**	−0.486**	−0.226**	−0.881**	−0.279**	0.514**
DO			−0.251**	−0.366**	−0.453**	−0.032	0.146*
TN				0.126	0.365**	0.304**	−0.507**
TP					0.240**	0.028	−0.029
CO_2						0.167*	−0.365**
DSi							−0.613**

*Correlation significant at the 0.05 level (2-tailed);
**Correlation significant at the 0.01 level (2-tailed).

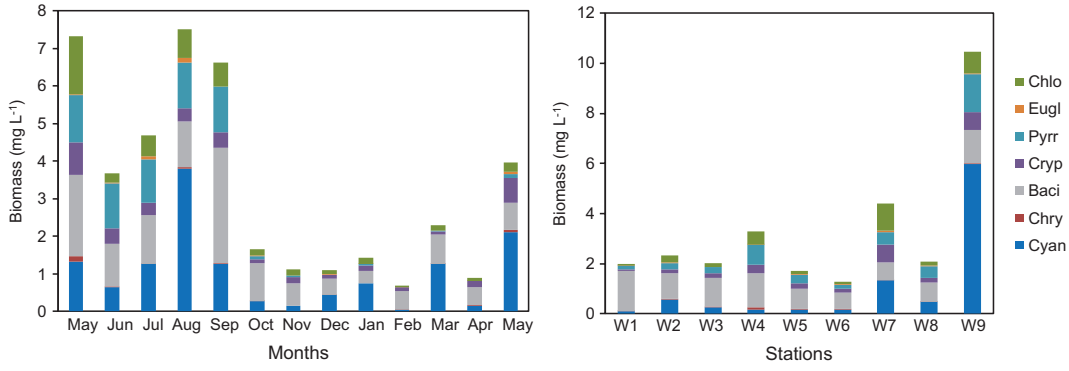

Figure 3. Average biomass (wet weight L^{-1}) of different phytoplankton groups in different stations on the Wujiang River from May 2011 to May 2012. Chlo = Chlorophyta; Eugl = Euglenophyta; Pyrr = Pyrrhophyta; Cryp = Cryptophyta; Baci = Bacillariophyta; Chry = Chrysophyta; Cyan = Cyanophyta. Station locations refer to Fig. 1.

river and thus is prone to phytoplankton growth. Algae assimilate CO_2 and release O_2, which can increase pH and DO. The significant positive correlations among Chl, pH, and DO indicated that photosynthesis is an important biological activity influencing water chemistry in the impounded river. By contrast, water chemistry in the natural river is usually controlled by chemical weathering of rocks and the mineralization of organic matter (Liu 2007).

According to the correlation analysis, water temperature was the key limiting factor for algal growth in these cascade reservoirs. An increase in T can enhance photosynthetic rates (Neori and Holm-Hansen 1982) and thus trigger faster phytoplankton growth. The assimilation of nutrients by the algae resulted in a decrease in concentration of TN, CO_2, and DSi in response to their significant negative correlations to Chl (Table 2). NO_3^- was the dominant species of TN (data not shown) and significantly correlated to Chl (r = −0.601, p < 0.01, n = 234); therefore, a negative relationship was found between TN and Chl. Freshwater ecosystems are often in a state of P limitation (Hecky and Kilham 1988). In this study, the TN:TP molar ratio was >50, which is indicative of P limitation (Guildford and Hecky 2000). Because the TP values were relatively high, however, and no significant correlation was found between TP and Chl (Table 2), P was probably not limiting in these reservoirs. The sensitivity analyses of BPANN models also confirmed this possibility (discussed later). Therefore, phytoplankton as a whole were not nutrient limited, but instead were thermal limited in the impounded Wujiang River.

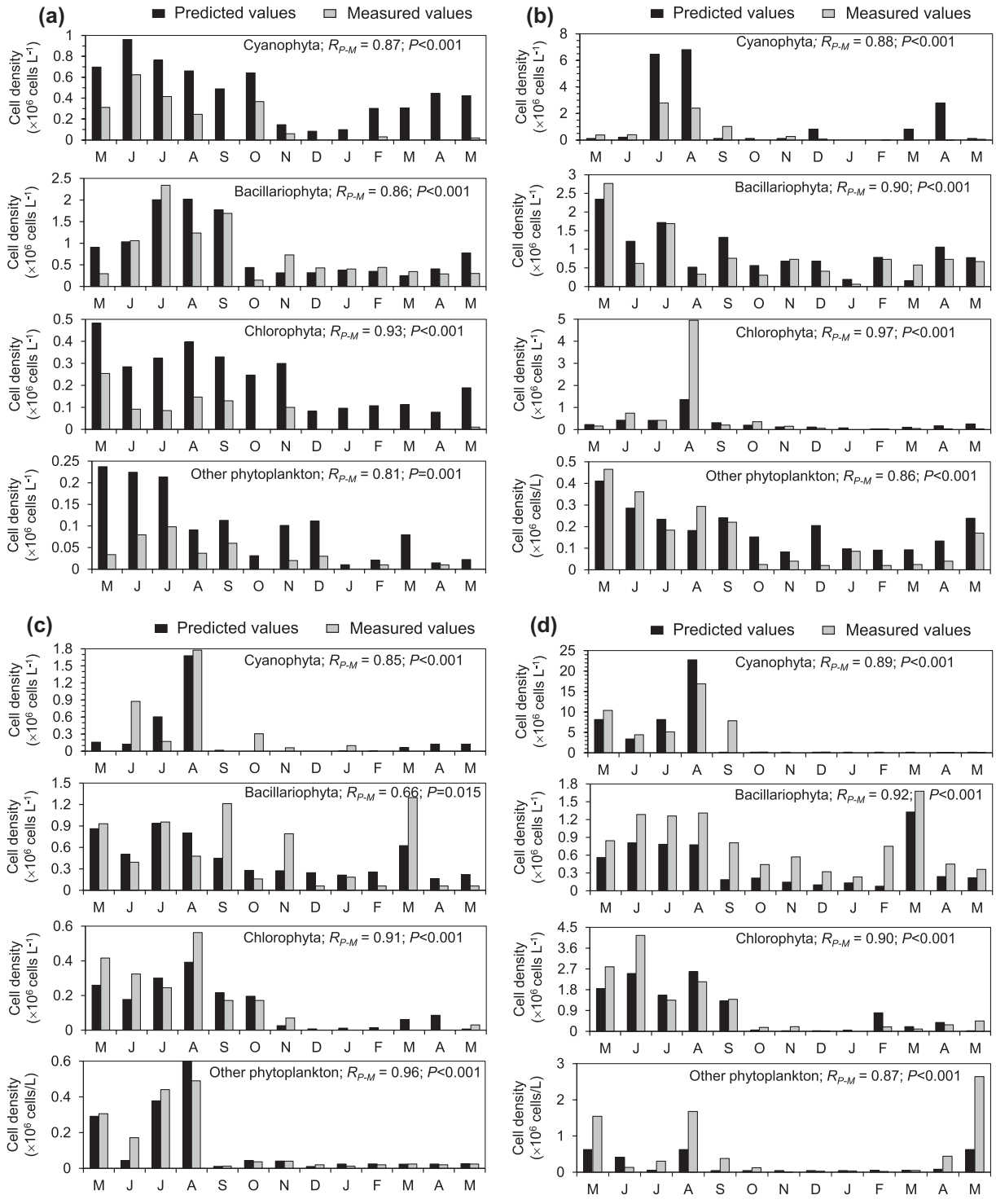

Figure 4. Validation of training results for different phytoplankton groups in the stations (a) W1, (b) W2, (c) W6, and (d) W7. Station locations refer to Fig. 1. $R_{P\text{-}M}$ is the correlation coefficient between the predicted values and measured values.

Factors driving phytoplankton dynamics based on BPANN models

BPANN models were used to simulate the dynamics of different phytoplankton phyla while previous studies were usually conducted with respect to a certain algal species (Recknagel 1997, Wei et al. 2001). The interspecific competition among different phyla and within the same phylum may complicate this simulation. Based on the time-lagged input parameters, our study demonstrated that the BPANN models could well predict time-series variation of phytoplankton groups, especially for the dominant algal phyla (Fig. 4).

Table 3. Sensitivity analyses of different phytoplankton groups related to changes of inputs by increasing 10% in stations W1, W2, W6, and W7. The names of dominant algal groups are bold. T = temperature; DO = dissolved oxygen; TP = total phosphorus; TN = total nitrogen; DSi = dissolved silicon. Sensitivity is calculated from the change of cell density divided by the original cell density. Inputs refer to T, pH, DO, CO_2, TN, TP, and DSi.

	T	pH	DO	CO_2	TP	TN	DSi
W1							
Cyanophyta (%)	−7.8	58.9	−11.8	−34.7	−1.1	2.6	4.7
Bacillariophyta (%)	−1.2	−16.5	−28.5	−28.7	−1. 3	7.3	8.1
Chlorophyta (%)	−0.5	−58.9	−13.5	−22.8	13.9	3.6	5.8
Other phytoplankton (%)	15.2	−133.2	−5.9	−8.3	−8.4	4.1	12.0
W2							
Cyanophyta (%)	41.3	−35.0	2.3	−34.6	0.1	−2.8	−0.4
Bacillariophyta (%)	6.5	−103.3	22.9	9.6	8.9	8.8	−34.1
Chlorophyta (%)	43.9	−45.4	−6.7	−2.3	−2.7	−8.3	0.8
Other phytoplankton (%)	−89.7	−103.9	−73.0	−24.1	−1.3	4.4	−13.9
W6							
Cyanophyta (%)	85.3	−113.9	75.1	57.8	−4.8	−11.3	5.7
Bacillariophyta (%)	35.6	183.0	42.9	6.8	−2.3	−8.0	0.6
Chlorophyta (%)	18.0	−89.9	106.0	12.1	−1.1	−13.7	11.3
Other phytoplankton (%)	111.6	7.4	21.9	−6.6	12.1	31.9	26.4
W7							
Cyanophyta (%)	188.6	−40.6	−51.9	−39.4	−2.6	−29.9	−2.5
Bacillariophyta (%)	−3.4	51.9	14.5	4.3	−4.7	−13.3	2.9
Chlorophyta (%)	8.6	−54.5	−5.5	−6.8	−0.0	−4.1	−1.4
Other phytoplankton (%)	13.0	8.5	0.4	11.6	0.1	−0.8	1.6

Table 4. Sensitivity analyses of different phytoplankton groups related to changes of inputs by decreasing 10% in the stations W1, W2, W6, and W7. The names of dominant algal groups are in bold. T = temperature; DO = dissolved oxygen; TP = total phosphorus; TN = total nitrogen; DSi = dissolved silicon. Sensitivity was calculated from the change of cell density divided by the original cell density. Inputs refer to T, pH, DO, CO_2, TN, TP, and DSi.

	T	pH	DO	CO_2	TP	TN	DSi
W1							
Cyanophyta (%)	−21.3	−140.8	8.9	−0.5	0.4	−3.5	−7.4
Bacillariophyta (%)	0.5	55.8	39.6	23.6	1.4	−7.6	−6.4
Chlorophyta (%)	−9.4	−9.0	6.3	−5.4	−15.2	−5.7	−6.8
Other phytoplankton (%)	−12.3	121.0	−5.6	3.8	9.8	−3.8	−12.6
W2							
Cyanophyta (%)	−28.8	34.8	22.7	36.3	−0.1	14.4	0.4
Bacillariophyta (%)	−16.8	79.7	−20.2	−14.6	−8.2	−9.0	36.1
Chlorophyta (%)	−20.0	142.9	7.8	28.9	2.6	9.6	−0.8
Other phytoplankton (%)	97.9	−126.4	57.7	24.0	1.1	−3.1	13.5
W6							
Cyanophyta (%)	−8.4	68.2	−76.8	27.3	5.6	65.9	−3.9
Bacillariophyta (%)	−34.5	18.7	−53.2	−7.0	2.2	8.5	1.3
Chlorophyta (%)	−29.3	−239.3	−139.0	−17.5	0.5	13.4	−13.5
Other phytoplankton (%)	−158.9	−939.1	−60.0	−10.9	−14.1	−38.0	−36.8
W7							
Cyanophyta (%)	−40.8	165.6	168.3	169.3	2.7	58.4	2.6
Bacillariophyta (%)	17.3	−15.4	−8.0	−3.6	5.7	20.2	−2.6
Chlorophyta (%)	−12.7	45.8	5.0	6.2	−0.0	4.1	1.4
Other phytoplankton (%)	11.6	−1.0	0.6	−1.4	−0.0	52.8	4.1

The sensitivity analyses of the BPANN models can be used to discern the main factors driving phytoplankton dynamics. The results indicated that changes of T and dominant algae were synchronous (Tables 3 and 4), suggesting that T was an important factor driving phytoplankton dynamics. The negative relationship between DSi and Bacillariophyta results from the assimilation of DSi by diatoms to build their frustules. Similarly, the low CO_2 concentrations when the biomass of Cyanophyta and Bacillariophyta was high resulted from uptake of CO_2 by photosynthesis. A close relationship between pH and CO_2 concentration was found (Table 2). In an ideal carbonate solution, pH is controlled by the ratio of $[CO_2]$:$[CO_3^{2-}]$, and a slight increase in $[CO_2]$ and an associated decrease in $[CO_3^{2-}]$ will cause a sharp decrease in pH. Therefore, the statistical results of pH as a key driving force reflected the effect of the carbon cycle on phytoplankton dynamics.

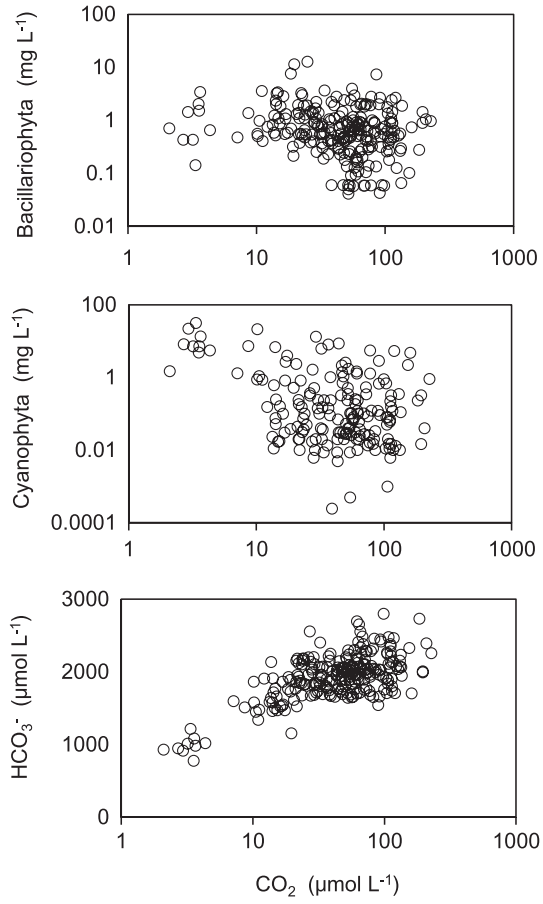

Figure 5. Scatter plots of biomass (wet weight L^{-1}) of Cyanophyta and Bacillariophyta and concentration of HCO_3^- vs. concentration of dissolved CO_2.

Biogeochemical mechanism of phytoplankton community succession in karst cascade reservoirs

The critical nutrient concentrations are specific for certain phytoplankton species because of their different pathways and strategies of using these nutrients, and thus variation of nutrient ratios can influence phytoplankton community structure (Grover 1989, Baldia et al. 2007, Wang et al. 2014). In karst cascade reservoirs, the spatial heterogeneity in phytoplankton community related to CO_2 and DSi biogeochemical cycle was notable. Algae have evolved CO_2-concentrating mechanisms (CCMs) to cope with low CO_2 availability, allowing them to take up HCO_3^- directly and/or indirectly by the conversion of HCO_3^- to CO_2 by extracellular carbonic anhydrase at the cell surface (Moroney and Ynalvez 2007). Species-specific differences in CCMs are great (Raven et al. 2012, Clement et al. 2017) and result in different responses of Bacillariophyta and Cyanophyta to the triggered CO_2 concentration. When CO_2 concentrations were less than ~10 μmol L^{-1}, the biomass of Bacillariophyta was relatively stable with decreasing CO_2 concentration, but that of Cyanophyta continued to bloom, accompanied by the obvious decrease in HCO_3^- concentration (Fig. 5). This finding suggests that during these conditions, Cyanophyta used HCO_3^- as an inorganic carbon source, whereas CCMs of Bacillariophyta were probably less efficient than Cyanophyta. Thus, Cyanophyta displaced Bacillariophyta as the dominant algae. The shift among the inorganic carbon species influenced pH (Wang et al. 2015), which explains the high pH sensitivity in Cyanophyta and Chlorophyta. Diatoms need Si to produce their frustules, and DSi concentration constrained the contribution of Bacillariophyta to the total phytoplankton (Fig. 6a). Biogenic Si has a much lower remineralization rate than organic N and P during organism decay (Muylaert et al. 2009). Thus, the recycling rates of N, P, and Si vary greatly (Koszelnik and Tomaszek 2008, Howarth et al. 2011), and eutrophication can enhance Si limitation and induce a shift from Bacillariophyta to Cyanophyta. Finally, CO_2 and DSi stoichiometry was in response to the succession from diatoms to nondiatoms (Fig. 6b).

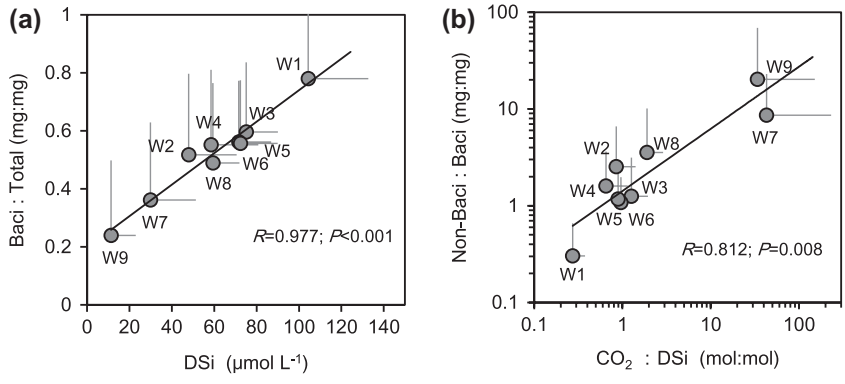

Figure 6. Scatter plots of (a) DSi vs. biomass of Bacillariophyta (Baci) to total phytoplankton (Total) ratio, and (b) CO_2:DSi vs. biomass of non-Bacillariophyta to Bacillariophyta ratio in different stations. Values were average and positive standard deviation. Station locations refer to Fig. 1.

Conclusions

Our results demonstrated that phytoplankton community structure exhibited clear variations across space and time in the impounded river, and BPANN models well predicted time-series variation of dominant algal abundance. Water temperature was an important limiting factor, and algal species succession was constrained by C and Si biogeochemical cycles in these karst cascade reservoirs.

Acknowledgements

This study was financially supported by the National Key R&D Program of China (2016YFA0601001), the National Natural Science Foundation of China (Grant Nos. U1612441 and 41473082), and CAS "Light of West China" Program. Comments from Stephen C. Maberly and another anonymous reviewer are thanked for greatly improving this manuscript.

Funding

This work was supported by the National Natural Science Foundation of China [grant number U1612441], [41473082]; National Key R & D Program of China [grant number 2016YFA0601001].

References

Baldia SF, Evangelista AD, Aralar EV, Santiago AE. 2007. Nitrogen and phosphorus utilization in the cyanobacterium *Microcystis aeruginosa* isolated from Laguna de Bay. Philippines. J Appl Phycol. 19:607–613.

Clement R, Jensen E, Prioretti L, Maberly SC, Gontero B. 2017. Diversity of CO_2-concentrating mechanisms and responses to CO_2 concentration in marine and freshwater diatoms. J Exp Bot. 68:3925–3935.

[EPA] Environmental Protection Agency. 1988. Environmental quality standard for surface water. State standard of the People's Republic of China (GB 3838-88). Environmental Protection Administration of China. Beijing (China): China Environmental Science Press.

Grover JP. 1989. Phosphorus-dependent growth kinetics of 11 species of freshwater algae. Limnol Oceanogr. 34:341–348.

Guildford SJ, Hecky RE. 2000. Total nitrogen, total phosphorus, and nutrient limitation in lakes and oceans: is there a common relationship? Limnol Oceanogr. 45:1213–1223.

Harris GP, Baxter G. 1996. Interannual variability in phytoplankton biomass and species composition in a subtropical reservoir. Freshwater Biol. 35:545–560.

Hecky RE, Kilham P. 1988. Nutrient limitation of phytoplankton in freshwater and marine environments: a review of recent evidence on the effects of enrichment. Limnol Oceanogr. 33:796–822.

Hillebrand H, Dürselen CD, Kirschtel D, Pollingher U, Zohary T. 1999. Biovolume calculation for pelagic and benthic microalgae. J Phycol. 35:403–424.

Howarth R, Chan F, Conley DJ, Garnier J, Doney SC, Marino1 R, Billen G. 2011. Coupled biogeochemical cycles: eutrophication and hypoxia in temperate estuaries and coastal marine ecosystems. Front Ecol Environ. 9:18–26.

Jeong KS, Kim DK, Joo GJ. 2006. River phytoplankton prediction model by artificial neural network: model performance and selection of input variables to predict time-series phytoplankton proliferations in a regulated river system. Ecol Inform. 1:235–245.

Koszelnik P, Tomaszek JA. 2008. Dissolved silica retention and its impact on eutrophication in a complex of mountain reservoirs. Water Air Soil Pollut. 189:189–198.

Lek S, Guegan JF. 1999. Artificial neural networks as a tool in ecological modelling, an introduction. Ecol Modell. 120:65–73.

Liu CQ. 2007. Earth surface biogeochemical processes and mass cycles: karstic catchment erosions and bioelements cycles in Southwest China. Beijing (China): Science Press. Chinese.

Maberly SC. 1996. Diel, episodic and seasonal changes in pH and concentration of inorganic carbon in a productive lake. Freshwater Biol. 35:579–598.

Markensten H, Moore K, Persson I. 2010. Simulated lake phytoplankton composition shifts toward cyanobacteria dominance in a future warmer climate. Ecol Appl. 20:752–767.

Moroney JV, Ynalvez RA. 2007. A proposed carbon dioxide concentration mechanism in *Chlamydomonas reinhardtii*. Eukaryot Cell. 6:1251–1259.

Muylaert K, Sanchez-Perez JM, Teissier S, Sauvage S, Dauta A, Vervier P. 2009. Eutrophication and its effect on dissolved Si concentrations in the Garonne River (France). J Limnol. 68:368–374.

Neori A, Holm-Hansen O. 1982. Effect of temperature on rate of photosynthesis in Antarctic phytoplankton. Polar Biol. 1:33–38.

Raven JA, Giordano M, Beardall J, Maberly SC. 2012. Algal evolution in relation to atmospheric CO_2: carboxylases, carbon-concentrating mechanisms and carbon oxidation cycles. Phil Trans R Soc B. 367:493–507.

Recknagel F. 1997. ANNA—artificial neural network model for predicting species abundance and succession of blue-green algae. Hydrobiologia. 349:47–57.

Reynolds CS, Wiseman SW, Godfrey BM, Butterwick C. 1983. Some effects of artificial mixing on the dynamics of phytoplankton populations in large limnetic enclosures. J Plankton Res. 5:203–234.

Rumelhart DE, Hinton GE, Williams RJ. 1986. Learning representations by back-propagating errors. Nature. 323:533–536.

Schabhuttl S, Hingsamer P, Weigelhofer G, Hein T, Weigert A, Striebel M. 2013. Temperature and species richness effects in phytoplankton communities. Oecologia. 171:527–536.

Serra T, Vidal J, Casamitjana X, Soler M, Colomer J. 2007. The role of surface vertical mixing in phytoplankton distribution in a stratified reservoir. Limnol Oceanogr. 52:620–634.

Wang B, Liu CQ, Peng X, Wang F. 2013. Mechanisms controlling the carbon stable isotope composition of phytoplankton in karst reservoirs. J Limnol. 72:127–139.

Wang B, Liu CQ, Wang F, Liu XL, Wang ZL. 2015. A decrease in pH downstream from the hydroelectric dam in relation to the carbon biogeochemical cycle. Environ Earth Sci. 73:5299–5306.

Wang B, Liu CQ, Maberly SC, Wang F, Hartmann J. 2016. Coupling of carbon and silicon geochemical cycles in rivers and lakes. Sci Rep. 6:35832. doi:10.1038/srep35832.

Wang F, Wang B, Liu CQ, Liu X, Gao Y, Zhang J, Li S. 2014. Changes in nutrient ratios and phytoplankton community structure caused by hydropower development in the Maotiao River, China. Environ Geochem Health. 36:595–603.

Wei B, Sugiura N, Maekawa T. 2001. Use of artificial neural network in the prediction of algal blooms. Water Res. 35:2022–2028.

Zhang ZS, Huang XF. 1991. Methods in freshwater plankton study. Beijing: Science Press. Chinese.